

Water Resources Research

RESEARCH ARTICLE

10.1029/2020WR027630

Key Points:

- Remote sensing was used to quantify the effects of topographic complexity on ecosystem productivity and its temporal variations
- Higher elevation, northeast aspects, and convergent valleys had higher long-term ecosystem productivity
- Ecosystem sensitivity to precipitation was higher in low elevation and highly productive areas and lower in convergent areas

Supporting Information:

- Supporting Information S1

Correspondence to:

X. Tai,
xiaonan.tai@njit.edu

Citation:

Tai, X., Anderegg, W. R. L., Blanken, P. D., Burns, S. P., Christensen, L., & Brooks, P. D. (2020). Hillslope hydrology influences the spatial and temporal patterns of remotely sensed ecosystem productivity. *Water Resources Research*, 56, e2020WR027630. <https://doi.org/10.1029/2020WR027630>

Received 1 APR 2020

Accepted 23 OCT 2020

Accepted article online 30 OCT 2020

Hillslope Hydrology Influences the Spatial and Temporal Patterns of Remotely Sensed Ecosystem Productivity

Xiaonan Tai^{1,2} , William R. L. Anderegg³ , Peter D. Blanken⁴ , Sean P. Burns^{4,5} , Lindsey Christensen¹, and Paul D. Brooks¹ 

¹Department of Geology and Geophysics, University of Utah, Salt Lake City, UT, USA, ²Department of Biological Sciences, New Jersey Institute of Technology, Newark, NJ, USA, ³School of Biological Sciences, University of Utah, Salt Lake City, UT, USA, ⁴Department of Geography, University of Colorado at Boulder, Boulder, CO, USA, ⁵National Center for Atmospheric Research (NCAR), Boulder, CO, USA

Abstract Prediction of ecosystem responses to a changing climate is challenging at the landscape to regional scale, in part because topography creates various habitats and influences ecosystem productivity in complex ways. However, the effects of topography on ecosystem function remain poorly characterized and quantified. To address this knowledge gap, we developed a framework to systematically quantify and evaluate the effects of topographic convergence, elevation, aspect, and forest type on the long-term (1986–2011) average and interannual variability of remotely sensed ecosystem productivity. In a forested watershed in the Rocky Mountains, spanning elevations from 1,800 to 4,000 m, we found a prevalent and positive influence of topographic convergence on long-term productivity. Interannual growing season productivity was positively related to precipitation, with higher sensitivity in low elevation and highly productive areas and lower sensitivity in convergent areas. Our findings highlight the influence of topographic complexity on both long-term and interannual variations of ecosystem productivity and have implications for understanding and prediction of ecosystem dynamics at hillslope to regional scales.

1. Introduction

Human-caused climate change is expected to result in more frequent and severe droughts in the 21st century, with potential consequences on ecosystem resilience and functions (Allen et al., 2015), water supply (Clow, 2010), and feedbacks to the atmosphere (Anderegg et al., 2019; Khanna et al., 2017). However, predicting ecosystem response to drought at landscape and regional scales remains challenging. Topography interacts with broader-scale climate regimes to create spatially heterogeneous fine-scale environments and their impacts on ecosystem function are complex and poorly understood. Systematic characterization and assessment of topographic influences on ecosystem productivity are urgently needed in order to reliably predict ecosystem dynamics and biological refugia within the next generation of Earth System Models (ESMs) (Fan et al., 2019; Fisher et al., 2017; McLaughlin et al., 2017).

Elevation, aspect, and ridge-valley convergence are three fundamental axes that topography exerts direct or indirect controls over the fine-scale abiotic conditions that vegetation experience within similar regional climatic regimes (Fan et al., 2019). By creating heterogeneous habitats that deviate from the regional climate, topography directly influences the abiotic resources necessary for plant function (Dobrowski, 2011; Moeslund, Arge, Bøcher, Dalgaard, Ejrnæs, et al., 2013). Elevation has long been recognized to be responsible for the systematic shifts in vegetation composition (Whittaker, 1967) and function (Goulden et al., 2012), through orographic lift and atmospheric lapse rates (Körner, 2007). Further, incident solar angle associated with hillslope aspects cause equator-facing aspects to receive greater solar radiation (Bennie et al., 2008), leading to higher surface temperatures. Both elevation and aspect can be directly incorporated into down-scaled climate products at finer resolution to account for their potential influences (Dobrowski, 2011; Z. Hoyleman et al., 2019). However, at smaller spatial scales such as hillslopes where the elevation and aspect per se do not fluctuate enough to cause variation in temperature or precipitation, the impact of microtopography is rather poorly understood (Moeslund, Arge, Bøcher, Dalgaard, & Svenning, 2013).

Topographically driven hydrologic processes (e.g., lateral flows of soil water and groundwater along convergence gradients from ridges to valleys) create drier hills and wetter valleys (Fan, 2015) and have emerged to be an important mechanism mediating the spatial pattern of biomass (Swetnam et al., 2017), leaf area index

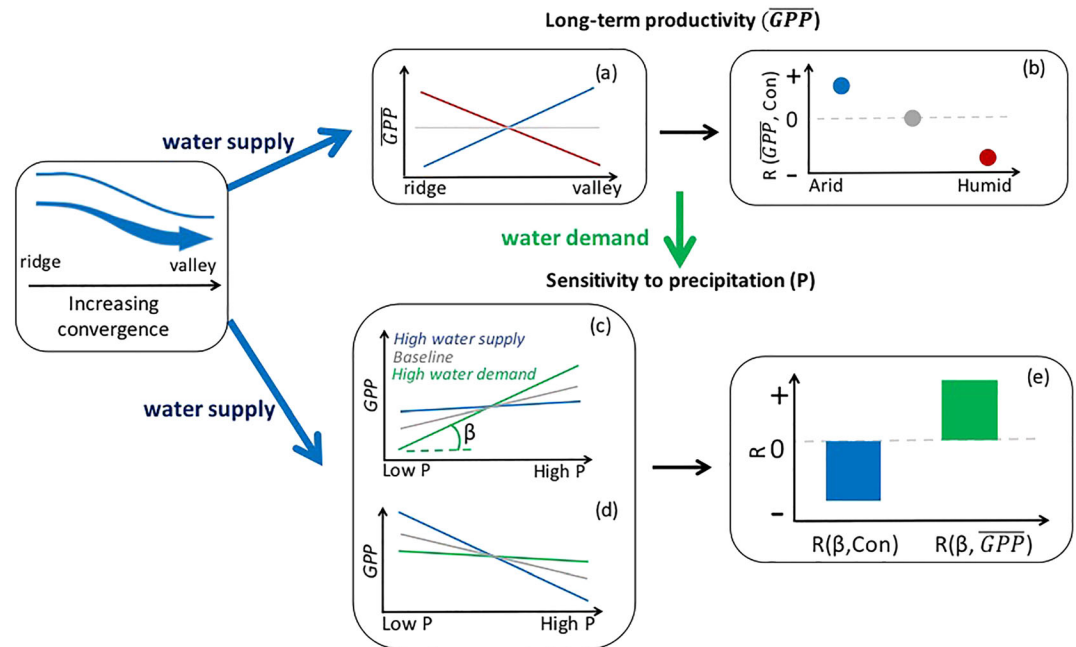


Figure 1. Conceptual framework evaluating topographic influences on the long-term mean ecosystem Gross Primary Productivity (\overline{GPP}) and the sensitivity to precipitation (β). We hypothesized topographic convergence to positively correlate with productivity in water-limited ecosystems (blue line in panel a) and negatively correlate with productivity in energy-limited ecosystems (red line in panel a). We also expected the influence of convergence on \overline{GPP} to shift from positive to negative along a hydroclimate gradient from arid to humid (b). Ecosystem sensitivity to precipitation can be quantified as the regression slope between annual GPP and precipitation (β in panels c and d). β will be positive in arid ecosystems (c) and negative in humid ecosystems (d). To assess the relative importance of convergence mediated water supply and \overline{GPP} mediated water demand (e), we expected a negative correlation between convergence and β when valleys having lower sensitivity (less positive or more negative β) to precipitation (blue bar in panel e). When sensitivity increased with higher water demand (more positive or less negative β), we expected positive correlations between sensitivity and \overline{GPP} (green bar in panel e).

(Bolstad et al., 2001; Hwang et al., 2009; Hwang et al., 2012), and drought-induced tree mortality at landscape scales (Schwantes et al., 2018; Simeone et al., 2018; Tai et al., 2017). Additionally, topographic convergence tends to align with soil processes (such as weathering and transport) and properties (such as texture and thickness), resulting in higher water storage capacity and further contributing to higher water availability in valleys (Famiglietti et al., 1998; Mackay, 2001; Moeslund, Arge, Bøcher, Dalgaard, Ejrnæs, et al., 2013; Rasmussen et al., 2011; Troch et al., 2015). Across the landscape, systematic variations of water availability driven by topographic convergence could result in a covarying spatial pattern of productivity along the ridge-valley gradient (Figure 1a), where valleys promote greater biomass and leaf area in water limited ecosystem (blue line in Figure 1a) through additional water supply (Hwang et al., 2009, 2012; Mackay, 2001; Mackay & Band, 1997; Swetnam et al., 2017; Thompson et al., 2011). In energy-limited ecosystems, biomass and leaf area may become smaller towards valleys (red line in Figure 1a), through reduced exposure to solar radiation or waterlogging of plant roots (Fan et al., 2019). Consequently, we expect the correlation between long-term productivity (e.g., accumulated biomass/leaf area) and topographic convergence to be positive where productivity is limited by water and negative where limited by energy (Figure 1b).

When the ecosystem is limited by water, topographic convergence could buffer ecosystem sensitivity to precipitation through increased *water supply* or increase the sensitivity through higher *water demand*. On one hand, plants in valleys may be more buffered from drought and have lower sensitivity to precipitation (blue line in Figure 1c), due to additional water supply through lateral hydrologic flow (Tai et al., 2018). On the other hand, plants in wet valleys tend to accumulate high biomass and/or leaf area from high productivity and have higher water demand and faster depletion of soil water during drought (Jump et al., 2017;

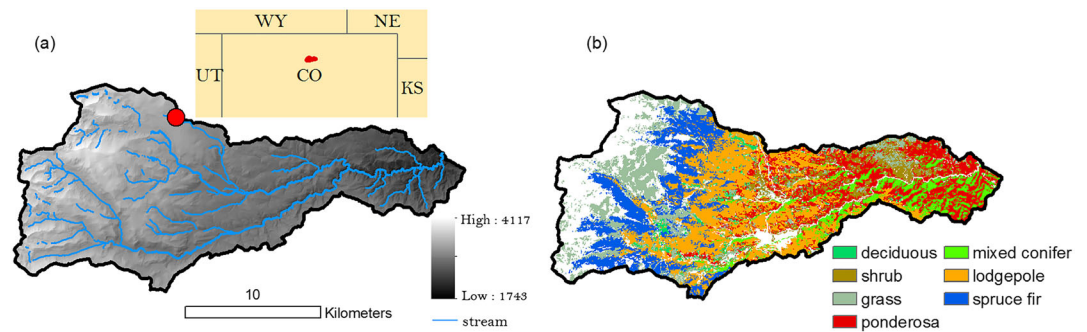


Figure 2. Maps of the study watershed a and its dominant ecosystem types (b). Red circle in (a) represents the location of Niwot Ridge eddy covariance flux tower, AmeriFlux: US-NR1 (<https://ameriflux.lbl.gov/sites/siteinfo/US-NR1#doi>). Areas not covered by vegetation are shown in white.

Tai et al., 2019), resulting in higher sensitivity to precipitation decline (green line in Figure 1c). When there is too much water, increased water supply might further reduce productivity (blue line in Figure 1d), whereas increased water demand might help release the anoxia stress and mediate productivity decline (green line in Figure 1d). Whether topographic convergence could buffer or aggravate vegetation from climatic water stress remains a large uncertainty in predicting ecosystem response to drought at landscape scales (Tague et al., 2019). Using the regression slope between productivity and precipitation (β in Figures 1c and 1d) to characterize ecosystem sensitivity to climatic water supply, the relative importance of water supply versus water demand could be assessed. A negative correlation between β and convergence (blue bar in Figure 1d) suggested convergent valleys have lower sensitivity to precipitation. A positive correlation between β and long-term productivity (green bar in Figure 1d) indicates places supporting higher productivity have higher sensitivity to precipitation.

Emergent vegetation patterns across the landscape can be readily observed from remote sensing and offered useful diagnostic tools to examine influence of physical and ecological processes (Hwang et al., 2009, 2012; Thompson et al., 2011). Physiologically meaningful products such as vegetation optical depth and solar-induced fluorescence have been used globally to understand ecosystem sensitivity to changing environment (Guan et al., 2015; Konings et al., 2017; Sun et al., 2018). But these products are typically limited to coarse spatial resolutions that cannot fully resolve hillslope-scale processes (Lutz et al., 2010; Millar et al., 2007). Landsat satellites provide three decades record with global coverage at a 30-m resolution and offer promising means to elucidate hydrological processes and ecosystem dynamics (Fan et al., 2019; Goulden & Bales, 2019; Z. H. Hoylman et al., 2018; Z. Hoylman et al., 2019; Liu et al., 2019).

In this study, we synthesized existing literature into a framework (Figure 1) that systematically quantifies topographic influence on ecosystem productivity and the relative importance of abiotic water supply and biotic water demands on ecosystem response to climatic water supply. We demonstrated this framework using multiple Landsat-derived indicators of productivity, in a forested watershed with steep topoclimate gradients spanning the lower and upper elevation limits of forest in the Rocky Mountains. Specifically, we ask, (1) how does topographic convergence relate to the long-term ecosystem productivity (Figure 1b)? (2) How does topographic influence on water supply interact with productivity mediated water demand in affecting ecosystem sensitivity to climate (Figure 1e)? And (3) where does topographic convergence matter the most for productivity and its sensitivity to climate, and do those areas occupy a significant portion of the watershed? Answers to these questions will improve our understanding of ecosystem function mediated by hillslope hydrological processes and provide empirical evidence informing the representation of hydrology in next generation of ESMs (Fan et al., 2019; Swenson et al., 2019).

2. Materials and Methods

2.1. Study Area

The study area is a forested watershed encompassing the Boulder Creek Critical Zone Observatory (Figure 2), located to the east side of the Continental divide and west of Boulder, Colorado. This watershed has an elevation gradient from 1,800 to 4,000 m above sea level (asl), with a mean elevation of 2,800 m asl.

Table 1
Pearson Correlation Between Statistics (Mean, Median, 75 Percentile, and Maximum) of Vegetation Metrics and Tower Measured GPP During July–September for the Period 1999–2011

	Median	Mean	Max	75 percentile
NIRv	0.71	0.80	0.76	0.83
NDVI	0.36	0.36	0.62	0.43
UMT_GPP	0.51	0.60	0.52	0.48

Note. Bold numbers are the statistics with highest correlation to tower GPP and used to represent growing season productivity for each grid cell.

The area of the entire watershed is 270 km², with 61.2 km² area covered by open water, permanent snow, and urban development. Mean annual precipitation ranges from 400 mm/yr to 1,200 mm/yr across elevation gradients. Mean growing season air temperature ranges from 1°C to 16°C, and the mean annual air temperature ranges from −4°C to 10°C (PRISM data). The watershed is dominated by vegetation communities that largely follow elevation gradients: Ponderosa Pine (*Pinus ponderosa*), Lodgepole Pine (*Pinus contorta*), and a mix of subalpine fir (*Abies lasiocarpa*), Engelmann spruce (*Picea engelmannii*).

2.2. Remotely Sensed Metrics for Ecosystem Productivity

To characterize vegetation productivity from remote sensing imagery, we used Normalized Difference Vegetation Index (NDVI), Near-infrared Reflectance of Vegetation (NIRv), and a Landsat-derived Gross Primary Production (GPP) data set. Although NDVI has been criticized for its limited physiological interpretation (Magney et al., 2019; Smith et al., 2019), it quantifies the amount and greenness of vegetation and has been correlated with leaf area index (Carlson & Ripley, 1997), evapotranspiration (Glenn et al., 2010; Goulden et al., 2012), and gross primary production (Gamon et al., 1995; Robinson et al., 2018; Tucker et al., 2001). NDVI has also been used as the benchmark of more physiologically relevant products such as vegetation optical depth (Li et al., 2017). NIRv, calculated as the product of NDVI and NIR reflectance, relates directly to the number of NIR photons reflected by plants and strongly correlates with GPP (Badgley et al., 2017, 2019). It also minimizes the effects of soil contamination and variable viewing geometry on satellite-derived spectra. The Landsat derived 16-day GPP product (UMT_GPP) (Robinson et al., 2018) has been used in a recent work to understand ecosystem climate sensitivity in western United States (Z. Hoyleman et al., 2019). UMT_GPP was based on the MODIS light-use efficiency GPP algorithm but replaced with finer resolution input data and spatially continuous and temporal regular Landsat NDVI composites developed using a smoothing and climatology driven gap filling approach (Robinson et al., 2017). We used all three GPP proxies to assess consistencies and disagreements that might arise from product differences.

We gathered NDVI and NIRv from Landsat 5 surface reflectance data using Google Earth Engine (Gorelick et al., 2017) at a 30 m resolution for the period 1986–2011 (until Landsat 5 was out of service). We did not use Landsat 7 to extend the study period, because homogenization between the two satellites is often required (Goulden & Bales, 2019) and might introduce additional uncertainty. A cloud removal algorithm was applied to each image to remove pixels that had a cloud likelihood score of 10% or higher (Zhu et al., 2015). Negative values were also excluded. Although UMT_GPP has longer record, we focused on the period 1986–2011 to be consistent with NDVI and NIRv. Further, since NIRv and NDVI are subjected to snow cover on the ground and intercepted by canopy during winter time and our study area is strongly influenced by snow, we focused on the snow-free period of 1 July to 30 September (Burns et al., 2015). A varying growing season length with elevation (Goulden et al., 2012) was not considered, limited by the temporal resolution and data gaps of Landsat imagery. For every year during the period 1 July to 30 September, mean, median, 75 percentile, and maximum values were calculated for NIRv, NDVI, and UMT_GPP. We identified the most representative statistics (mean, median, 75 percentile, or maximum) by comparing against the mean growing season GPP measured from an eddy covariance flux tower (Niwo Ridge, AmeriFlux: US-NR1), extracted from tier 1 FLUXNET 2015 (Pastorello et al., 2017) and selected the statistics achieving the highest Pearson correlation (bold numbers in Table 1). We then calculated 75 percentile NIRv, maximum NDVI, and mean UMT_GPP during July–September for each year, generating three annual time series of ecosystem productivity at every 30 m pixel.

2.3. Topography and Climate Data

A digital elevation model (DEM) at 30-m resolution was downloaded from National Elevation Data Set. Indices of aspect and topographic wetness index (TWI) were computed from DEM. TWI combines upslope accumulated area and local slope and has been widely used as a proxy for water availability induced by lateral drainage (Famiglietti & Wood, 1994; Hwang et al., 2012; Tai et al., 2017), although the correlation strength can vary depending on antecedent moisture conditions (Western et al., 1999). A 30-m resolution map of dominant ecosystem types was extracted from National GAP Land Cover Data (Lowry et al., 2007),

to identify four forest dominated ecosystems in study watershed: ponderosa, mixed conifer, lodgepole, and spruce-fir forests. Monthly precipitation and temperature at a spatial resolution of 4 km were obtained from the Parameter-elevation Relationships on Independent Slopes (PRISM) data set (Daly et al., 2008) during the period 1984–2011. We also used climatic water deficit (CWD), calculated as potential evapotranspiration minus actual evapotranspiration based on Penman-Monteith approach and Thornthwaite-Mather climatic water-balance model (Abatzoglou et al., 2018). Precipitation, temperature, and CWD were aggregated to annual mean or sum on a water-year basis (October–September). Although winter precipitation is likely important source of tree water supply in snow-dominated environment (Martin et al., 2018), we resorted to annual precipitation based on previous research in the study area (Adams et al., 2014; Hu, Moore, Burns, et al., 2010). Further, we compared the amount of variance in GPP explained by annual versus winter precipitation and found remotely sensed GPP indices were better explained by annual precipitation (supporting information Figure S1). Both PRISM and CWD data sets have a resolution of 4 km, and different grid cells showed similar interannual variations over time, although their absolute magnitude shifted with elevation (Figure S2). We averaged all 4 km grid cells falling within the watershed and used the watershed-wide mean climate in the following analysis. Further, we repeated the analysis using distributed climate series at 4 km resolution and found similar result using watershed-wide climate series (Figure S3).

2.4. Analysis

For every pixel, we calculated the long-term average productivity during 1986–2011, based on three remotely sensed indicators of vegetation productivity (noted as \overline{NIRv} , \overline{NDVI} , and $\overline{UMT_GPP}$, respectively). Further, we performed linear regressions between productivity and precipitation for every 30 m pixel using 26 years of record (1986–2011). We also explored fitting segmented regression between productivity and precipitation and found little improvement over linear regression. Thus, linear regression was used in the following analysis. Both productivity metrics and precipitation were standardized to z -scores (subtracted the mean and divided by standard deviation), allowing direct comparisons across locations, regardless of units and magnitudes (Z. Hoylman et al., 2019; Konings et al., 2017). We used the regression slope as a measure of ecosystem sensitivity to climatic water supply, with higher values indicating greater sensitivity. This simple metric provides the first-order characterization of vegetation response to precipitation and has been applied in several recent studies (Anderegg et al., 2018; Baldocchi et al., 2019; Z. Hoylman et al., 2019; Konings et al., 2017). Following the practice in a previous study (Z. Hoylman et al., 2019), we did not remove regressions with insignificant slope coefficients (i.e., p -values > 0.05) in order to preserve pixels with slopes close to 0 (insensitive pixels). To corroborate our results, we repeated the same analysis using CWD, which accounted for both climatic water supply and demand. Further, since annual temperature and precipitation were weakly correlated in our study area (Pearson's $r = 0.24$, Table S1), we also ran regressions using both temperature and precipitation as predictors to evaluate their separated effects.

We used Spearman correlation to assess the influence of topographic convergence on the long-term mean and sensitivity of productivity. To minimize the potential influence of confounding factors such as ecosystem types, elevation, and aspect, we discretized the entire watershed into four dominated forests (ponderosa, mixed conifer, lodgepole, and spruce-fir). Within each ecosystem type, we further divided the data into 10 percentiles based on elevation, and two categories of aspect: $135^\circ \sim 315^\circ$ and $-45^\circ \sim 135^\circ$ measured clockwise from north (SW and NE hereafter). Within bins of the same ecosystem and similar elevations and aspects, we correlated TWI and mean productivity to evaluate the influence of convergence on long-term productivity (Figures 1a–1c). We also correlated sensitivity with TWI and with mean productivity, respectively, to assess the relative importance of water supply versus water demand (Figures 1c and 1d). We evaluated if the correlation is significantly different from zero using one-sample t test. We also evaluated if the strength of correlation varied with elevation using linear regressions. Spatial data processing and statistical analyses were carried out in R (R Core Team, 2015).

3. Results

3.1. Long-Term Ecosystem Productivity

The long-term mean of ecosystem productivity was spatially heterogeneous, based on different remote sensing metrics of NIRv, NDVI, and UMT_GPP (Figures 3a–3c). Broadly, productivity increased from low to high elevation and from SW to NE aspects (Figures 3d–3f). Ponderosa had much lower \overline{NDVI} and

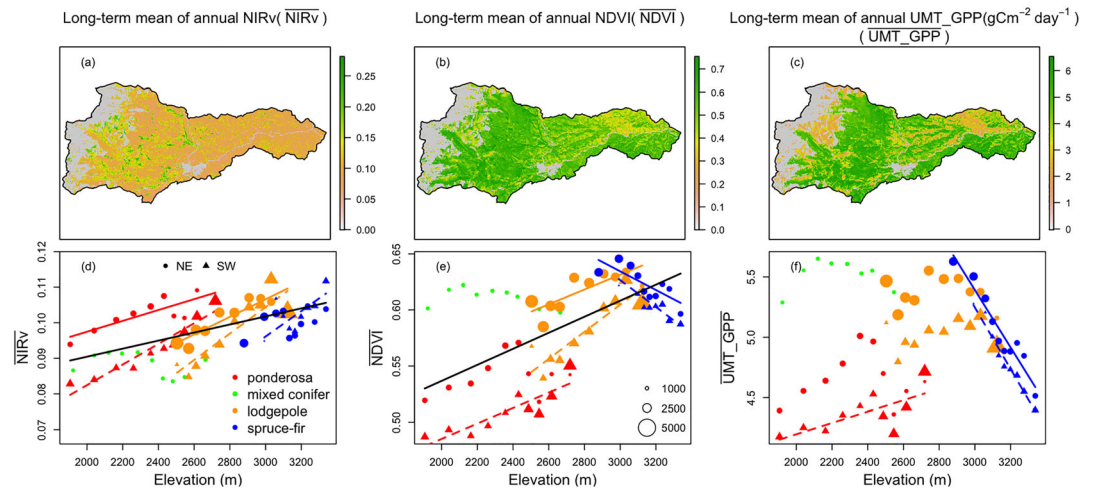


Figure 3. Maps of the long-term average of growing-season productivity for the period 1986–2011 based on remotely sensed metrics of NIRv (a), NDVI (b), UMT_GPP (c). Areas not covered by vegetation, and with more than 10% of missing data were filtered and shown in gray. (d)–(f) The scatterplots of NIRv (d), NDVI (e), and UMT_GPP (f) versus elevation. The y-axis represented the mean productivity for different bins of forest types (color), elevation, and aspect (symbol). Symbol size is proportional to the number of 30 m pixels within each bin. Regression lines were shown for each forest type (color) and aspect group (solid for NE aspect and dashed for SW aspect) when p -value < 0.05. Black solid line is the regression for all data points.

$\overline{UMT_GPP}$, likely due to the typical canopy openness of ponderosa pine forests. Within ecosystems, ponderosa productivity increased with elevation, particularly on SW facing aspects (red triangles and red dashes in Figures 3d–3f). Lodgepole also had increasing productivity with elevation, although $\overline{UMT_GPP}$ showed no significant trend ($p = 0.05$). In spruce-fir forest, NDVI and UMT_GPP decreased with elevation, while \overline{NIRv} showed slight increase with elevation.

3.2. Influence of Topographic Convergence on Long-Term Ecosystem Productivity

Across different elevation, aspect, and ecosystem types, TWI was positively correlated with productivity (Figure 4), except for a few patches of spruce-fir and ponderosa. The correlation strength declined with elevation in the lower elevation range and increased with elevation in the higher elevation range.

3.3. Interannual Sensitivity of Productivity to Precipitation

Over the 26 years of record used in this analysis, we found that productivity was positively related to precipitation for most pixels, based on all three metrics (Figures 5a–5c). The sensitivity (β) declined as elevation increased but remained positive (Figures 5d–5f), except for NIRv in two spruce-fir patches. The influence of

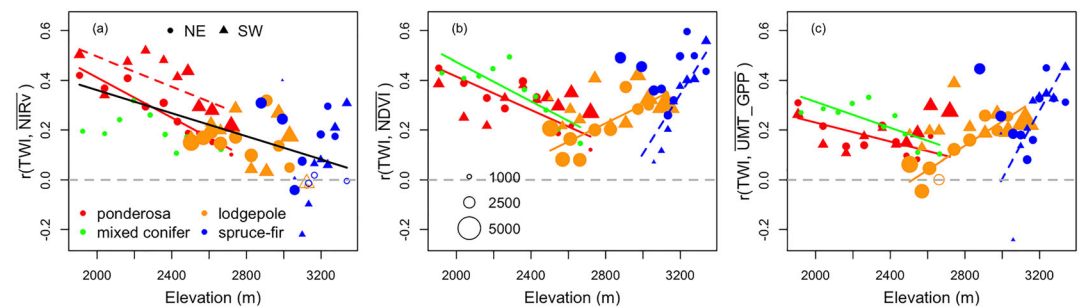


Figure 4. Spearman correlation between TWI and productivity versus elevation within different patches of ecosystem type (color), elevation, and aspect (dots vs. triangle), based on remotely sensed metrics of NIRv (a), NDVI (b), and UMT_GPP (c). Symbol size was proportional to the number of 30 m pixels within each bin. Significant correlations ($p < 0.05$) were shown as solid symbols and insignificant correlations ($p > 0.05$) were shown as open symbols. Trend lines denote a significance level of $p < 0.05$. Line colors represent different ecosystem types, solid lines represent NE aspect, and dashed lines represent SW aspect. Black solid lines represent regression across all data points.

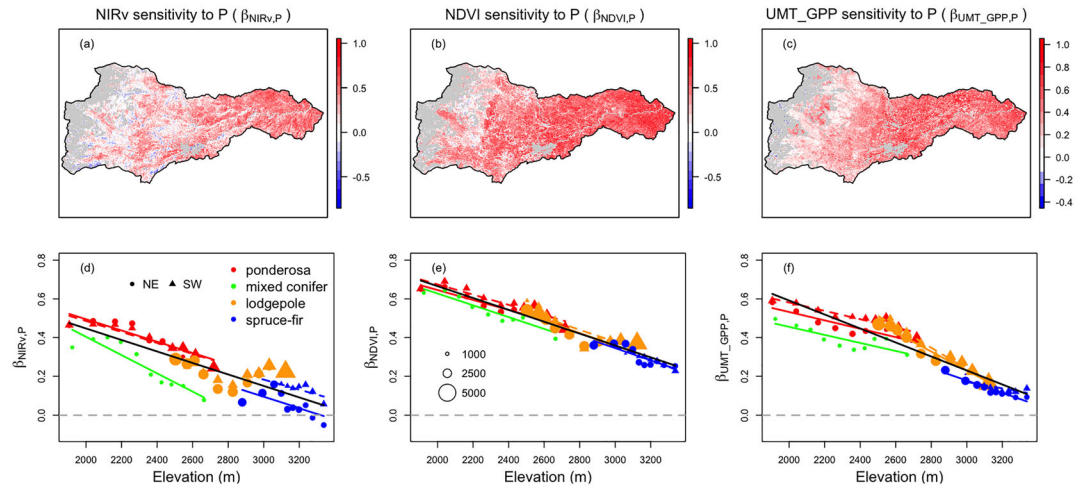


Figure 5. Maps of ecosystem sensitivity to precipitation (β) derived using NIRv (a), NDVI (b), UMT_GPP (c) to annual precipitation (P) for the period 1986–2011. Areas not covered by vegetation, and with more than 10% of missing data were filtered and shown in gray. (d)–(f) The sensitivity of NIRv (d), NDVI (e), and UMT_GPP (f) to precipitation versus elevation. Sensitivity was defined as the regression slope between productivity and precipitation, denoted as $\beta_{\text{NIRv}, P}$, $\beta_{\text{NDVI}, P}$, and $\beta_{\text{UMT_GPP}, P}$, respectively. They-axis represented the mean sensitivity of patches with same or similar forest types (color), elevation, and aspect (symbol). Symbol size was proportional to the number of 30 m pixels within each bin. Regression lines were shown for each forest type (colored lines) and aspect group (solid for NE aspect and dashed for SW aspect) when p -value < 0.05 . Black solid line is the regression for all data points.

aspect and ecosystem types appeared small compared to elevation. These findings were robust after accounting for temperature or using climatic water deficit to derive sensitivity (Figure S4).

3.4. Influence of Topographic Convergence on Ecosystem Sensitivity to Precipitation

Across different ecosystems, elevations, and aspects, the correlation between TWI and sensitivity to precipitation (β) was significantly lower than zero ($p = 0.05$), with the only exception of UMT_GPP (blue boxes in Figure 6). The correlation between long-term productivity and β was significantly higher than zero ($p = 0.05$) (green boxes in Figure 6). Comparing the relative importance of TWI versus long-term productivity on β , long-term productivity had stronger correlation in most landscape patches (Figure 6), although the spatial pattern varied by remote sensing metrics (Figure S5).

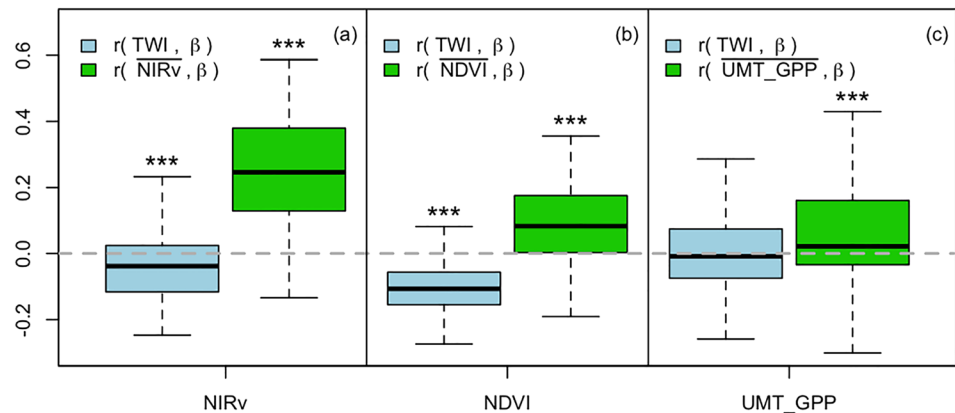


Figure 6. Boxplot of Spearman correlation between sensitivity to precipitation (β) and TWI (light blue boxes) and the correlation between β and long-term productivity (green boxes), using NIRv (a), NDVI (b) and UMT_GPP (c). The correlation was calculated within patches of same ecosystem types and similar elevations and aspect groups. One-sample t -test was used to evaluate if the correlation was significantly different from 0, with $***p < 0.01$.

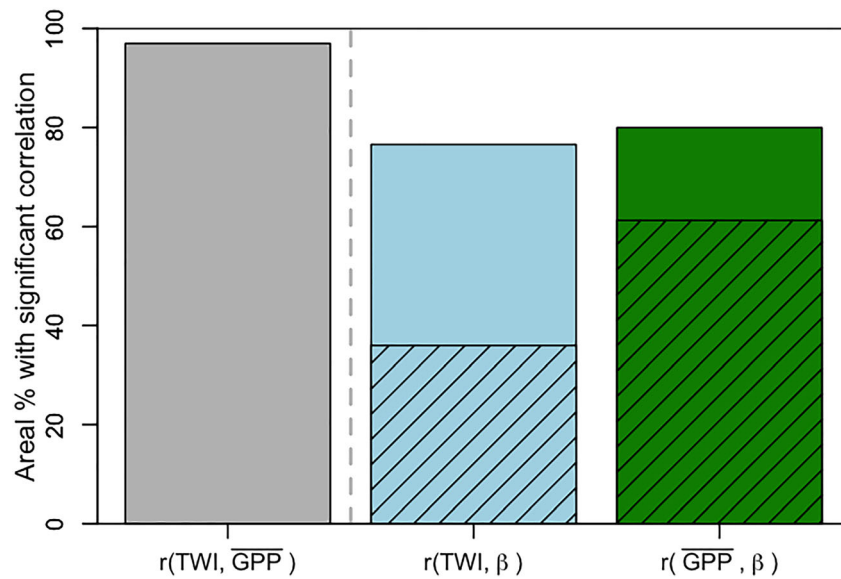


Figure 7. Areal fractions of the forested areas within the watershed that demonstrated significant ($p < 0.05$) spearman correlations between topographic convergence and long-term productivity $r(\text{TWI}, \overline{\text{GPP}})$ (gray bar), between topographic convergence and sensitivity $r(\text{TWI}, \beta)$ (blue bar), and between long-term productivity and sensitivity $r(\overline{\text{GPP}}, \beta)$ (green bar). Areal fractions were reported as the average of fractions derived using different remote sensing metrics of ecosystem productivity. Hatched blue bar represented areal fraction of patches with stronger influence of TWI than $\overline{\text{GPP}}$, and hatched green bar represented areal fraction of patches with stronger influence of $\overline{\text{GPP}}$ than TWI.

3.5. Areas Influenced by Topographic Convergence Across the Watershed

Across the watershed, ~96% of forested area showed significant correlation ($p < 0.05$) between TWI and long-term productivity ($\overline{\text{GPP}}$) (Figure 7, gray bar); 76% area demonstrated significant correlation between TWI and sensitivity (β) (Figure 7, blue bar); and 80% area had significant correlation between $\overline{\text{GPP}}$ and β (Figure 7, green bar). TWI showed stronger influence on β for 36% of the area while $\overline{\text{GPP}}$ had stronger control of β in 60% of the landscape (hatched bars in Figure 7).

4. Discussion

Interaction between hydrological and ecological processes at watershed scales has been examined for decades (Z. H. Hoylman et al., 2018; Z. Hoylman et al., 2019; Hwang et al., 2009, 2012; Mackay, 2001; Mackay & Band, 1997; Swetnam et al., 2017) and are becoming increasingly critical for predicting ecosystem response to novel environments and anticipated future drought (Clark et al., 2015; Fan et al., 2019). In this study, we synthesized previous evidences into a framework that quantifies the influence of topography on the long-term ecosystem productivity and expanded upon previous work by assessing the relative importance of abiotic water supply and biotic water demand on the temporal variations of ecosystem productivity to climatic water supply. This framework can be transferable to different time scales and different measures of ecosystem productivity. This framework was demonstrated in a semiarid, forested watershed with steep topoclimate gradients and multiple forest types to better understand the relative importance of different controls on ecosystem productivity across the landscape. Based on multiple remotely sensed metrics, we found strong evidence supporting the positive influence of topographic convergence on long-term productivity for ~96% of forested area (Figures 4 and 7). Growing season productivity was higher in years with higher precipitation and the sensitivity strongly decreased with elevation (Figure 5). Ecosystem sensitivity to precipitation was lower in convergent areas and higher in areas with higher long-term productivity (Figure 6). While these results were robust, we also discussed disagreements among different remote sensing metrics and highlighted opportunities for future work.

4.1. Topographic Signature on the Long-Term Mean of Ecosystem Productivity

Vegetation patterns systematically varied with topographic gradients. Ecosystem productivity was higher in higher elevations with NE aspects (Figure 3) and convergent areas (Figure 4). This is consistent with previous studies using NDVI (Hwang et al., 2012), enhanced vegetation index (Z. H. Hoylman et al., 2018), and Lidar-derived aboveground biomass (Swetnam et al., 2017). These evidences suggested the prevalent influence of water availability on plant productivity and biomass accumulation at watershed scales. Similarly, water availability best explained tree height in a global analysis (Klein et al., 2015). In high elevation spruce-fir forests, NDVI and UMT_GPP decreased, while NIRv increased with elevation. This could reflect the different properties of vegetation captured by various remote sensing metrics. While NDVI and UMT_GPP reflected the amount of vegetation on the ground, NIRv minimized the effects of vegetation amount and captured the photosynthetic activity per unit vegetation cover (Badgley et al., 2017). It is possible that in these spruce-fir forests, photosynthetic activity increased with elevation, while vegetation cover decreased with elevation.

The influence of topographic convergence on productivity varied with elevation (Figure 4). Its influence declined with elevation in ponderosa pine forest, likely due to the gradual release of water limitation with elevation (Körner, 2007). We initially hypothesized productivity to be negatively influenced by convergence in high elevations due to anticipated energy limitation close to tree line (Figure 1b). However, this was not supported. Correlations between productivity and TWI were mostly positive and became stronger with elevation in spruce-fir (Figure 4). Spruce-fir productivity was higher in NE aspect and convergent areas that are likely to be wetter and in warmer, lower elevations. This might suggest these forests were limited by both energy (Bigler, 2016; Bonan, 2015; Kane et al., 2014; Whittaker, 1967) and water (Hu, Moore, Burns, et al., 2010; Hu, Moore, Riveros-Iregui, et al., 2010; Trujillo et al., 2012). Another possible explanation could be higher nutrient on NE aspects and convergent areas supported higher productivity (Moeslund, Arge, Bøcher, Dalgaard, Ejrnæs, et al., 2013; Smith et al., 2017; Weintraub et al., 2015, 2017).

4.2. Topographic Influence on Ecosystem Sensitivity to Climatic Water Supply

We found ecosystem productivity was positively related to precipitation (Figure 5), negatively related to air temperature and climatic water deficit (Figure S4). This highlights the importance of annual water supply on growing season productivity and is consistent with a previous study in the upper elevation of the watershed showing photosynthesis could be limited by water in late growing season (Hu, Moore, Burns, et al., 2010). However, a recent continental study based on annual net primary productivity (NPP) showed energy limitation in our study area (Z. Hoylman et al., 2019). The disagreement might be attributed to our focus on growing season GPP in this current study. Plants are more likely to be limited by water in late growing season and by energy in early season or winter time. Another possible explanation could be the algorithms used to derive GPP from Landsat NDVI and climate products (Robinson et al., 2018), which includes temperature-driven GPP functions that might have led to overly strong sensitivity to temperature. Simple linear regressions showed UMT_GPP responded positively to temperature (Figure S4i) while both NIRv and NDVI, which do not rely on temperature-sensitivity functions, responded negatively (Figure S4g,h). Similarly, regression using Niwot Ridge tower data demonstrated positive slope for precipitation and negative slope for temperature.

Although different remote sensing metrics produced slightly different estimates, we found significant evidences that convergent areas had lower sensitivity to precipitation, mostly in low elevations (blue boxes in Figure 6). This supported the hypothesis that plants in valleys receive higher water supply and experience less productivity decline when precipitation is low, through lateral flow or soil water storage (Z. Hoylman et al., 2019; Tai et al., 2018, 2019). Areas with higher \overline{GPP} had higher sensitivity to precipitation (green boxes in Figure 6), consistent with the expectation that greater productivity accumulate and translate into higher biomass, leaf area, and higher water demand and result in faster depletion of water storage during drought (Jump et al., 2017; Tai et al., 2019). Comparing the relative importance, \overline{GPP} appeared to have stronger correlation with sensitivity than TWI (Figure 6) and a larger fraction of the watershed was prevalently influenced by \overline{GPP} than TWI (hatched bars in Figure 7), suggesting the stronger influence of biotic water demand compared to abiotic water supply. These findings fell in line with the phenomena that has reported places supporting higher leaf area tend to have higher tree mortality (Goulden & Bales, 2019; Jump et al., 2017).

$r(\text{TWI}, \beta)$ and $r(\overline{\text{GPP}}, \beta)$ did not demonstrate systematic spatial patterns across the watershed as $r(\text{TWI}, \overline{\text{GPP}})$ (Figure S5, Figure 4). This might be an indication of the complex interactions of various abiotic and biotic factors underlying ecosystem sensitivity to precipitation (β), in addition to TWI-mediated water supply and $\overline{\text{GPP}}$ -mediated water demand. For example, trees growing on ridge tops might develop deeper roots that allow them to tap into water stored in bedrock (Fan et al., 2017), making them more resistant rather than more sensitive to drought. Quantifying interspecific and intraspecific variations of plant physiological traits across gradients of abiotic environments of water table, nutrient supply, and evaporative demand remains research priority, in order to understand how they combine to influence ecosystem-level response to drought (Cosme et al., 2017; Hirota & Oliveira, 2020; Oliveira et al., 2019).

4.3. Methodological Considerations

Although our results were generally consistent among different remotely sensed productivity indicators and climate variables, there are a number of caveats that warrant further investigations. First, we selected remote sensing metrics that were best correlated with productivity observed from an eddy covariance tower located in the upper range of the study watershed. It is possible that the optimal indices at tower site might not be representative at other sites. Second, although our conceptual framework is generally applicable to both water and energy-limited environment, our case study was focused in a semiarid watershed with water limitation during growing season. It is worth noting that different results might be arrived when applying our conceptual framework to other systems, and modification or rejection of our initial hypothesis might be needed. Third, we used annual time scales in our case study, whereas subannual or multiyear time scales might be invoked when applying to different systems. Annual climate may not be the optimal time scale when ecosystems are more responsive to short-term events such as storms (Tromp-van Meerveld & McDonnell, 2006; Zscheischler et al., 2014) or multiyear droughts (Goulden & Bales, 2019).

5. Conclusions

We demonstrated a framework of joint topography-climate-vegetation analysis to characterize and quantify the influence of hydrological and ecological processes underlying vegetation dynamics across heterogeneous landscapes. The conceptual framework provides a set of testable hypotheses and can be easily transferrable to other systems or temporal scales. Results from a case study revealed quantitative disagreements when using different remote sensing products and highlighted the need to combine multiple lines of evidences to derive robust conclusions. We conclude that topographic convergence is closely related to ecosystem function through processes mediating resource availability and plant water demand and will likely be important in determining ecosystem dynamics to future climate conditions. Our study adds to the growing body of literature leveraging globally available remote sensing to identify hydrological refugia in the face of a changing climate and answers a broader call for comprehensive evaluation of terrain structure on vegetation distribution and functions (Fan et al., 2019).

Data Availability Statement

All data used in this study were publicly available online. Eddy covariance data were extracted from FLUXNET2015 (<https://fluxnet.org/data/fluxnet2015-dataset/>). Climate data were downloaded from PRISM (<https://prism.oregonstate.edu/>) and TerraClim (<http://www.climatologylab.org/terraclim.html>). Landsat data were downloaded from Google Earth Engine (<https://earthengine.google.com/>).

References

- Abatzoglou, J. T., Dobrowski, S. Z., Parks, S. A., & Hegewisch, K. C. (2018). TerraClimate, a high-resolution global dataset of monthly climate and climatic water balance from 1958–2015. *Scientific Data*, 5(1), 170191. <https://doi.org/10.1038/sdata.2017.191>
- Adams, H. R., Barnard, H. R., & Loomis, A. K. (2014). Topography alters tree growth-climate relationships in a semi-arid forested catchment. *Ecosphere*, 5(11), art148. <https://doi.org/10.1890/es14-00296.1>
- Allen, C. D., Breshears, D. D., & McDowell, N. G. (2015). On underestimation of global vulnerability to tree mortality and forest die-off from hotter drought in the Anthropocene. *Ecosphere*, 6(8), 1–55. <https://doi.org/10.1890/es15-00203.1>
- Anderegg, W. R., Konings, A. G., Trugman, A. T., Yu, K., Bowling, D. R., Gabbitas, R., et al. (2018). Hydraulic diversity of forests regulates ecosystem resilience during drought. *Nature*, 561. <https://doi.org/10.1038/s41586-018-0539-7>
- Anderegg, W. R., Trugman, A. T., Bowling, D. R., Salvucci, G., & Tuttle, S. E. (2019). Plant functional traits and climate influence drought intensification and land-atmosphere feedbacks. *Proceedings of the National Academy of Sciences*, 116, 201,904,747. <https://doi.org/10.1073/pnas.1904747116>

Acknowledgments

We would like to thank Dr. John Sperry (University of Utah) for providing feedbacks on an earlier version of the manuscript. Funding from National Science Foundation (NSF) through grant IOS 1450650 is acknowledged. W. R. L. A. acknowledges funding from the David and Lucille Packard Foundation, NSF Grants 1714972 and 1802880 and the USDA National Institute of Food and Agriculture, Agricultural and Food Research Initiative grant no. 2018-67019-27850. The National Center for Atmospheric Research (NCAR) is sponsored by NSF. The statements made in this manuscript reflect the views of the authors and do not necessarily reflect the views of the funding agencies.

- Badgley, G., Anderegg, L. D., Berry, J. A., & Field, C. B. (2019). Terrestrial gross primary production: Using NIRV to scale from site to globe. *Global Change Biology*, 25(11), 3731–3740. <https://doi.org/10.1111/gcb.14729>
- Badgley, G., Field, C. B., & Berry, J. A. (2017). Canopy near-infrared reflectance and terrestrial photosynthesis. *Science Advances*, 3(3), e1602244. <https://doi.org/10.1126/sciadv.1602244>
- Baldocchi, D., Dralle, D., Jiang, C., & Ryu, Y. (2019). How much water is evaporated across California? A multiyear assessment using a biophysical model forced with satellite remote sensing data. *Water Resources Research*, 55, 2722–2741. <https://doi.org/10.1029/2018WR023884>
- Bennie, J., Huntley, B., Wiltshire, A., Hill, M. O., & Baxter, R. (2008). Slope, aspect and climate: Spatially explicit and implicit models of topographic microclimate in chalk grassland. *Ecological Modelling*, 216(1), 47–59. <https://doi.org/10.1016/j.ecolmodel.2008.04.010>
- Bigler, C. (2016). Trade-offs between growth rate, tree size and lifespan of mountain pine (*Pinus montana*) in the Swiss National Park. *PLoS ONE*, 11(3), e0150402. <https://doi.org/10.1371/journal.pone.0150402>
- Bolstad, P. V., Vose, J. M., & McNulty, S. G. (2001). Forest productivity, leaf area, and terrain in southern Appalachian deciduous forests. *Forest Science*, 47(3), 419–427. <https://doi.org/10.1093/forestscience/47.3.419>
- Bonan, G. (2015). *Ecological climatology: Concepts and applications*. Cambridge: Cambridge University Press.
- Burns, S., Blanken, P., Turnipseed, A., Hu, J., & Monson, R. (2015). The influence of warm-season precipitation on the diel cycle of the surface energy balance and carbon dioxide at a Colorado subalpine forest site. *Biogeosciences*, 12, 7349–7377. <https://doi.org/10.5194/bg-12-7349-2015>
- Carlson, T. N., & Ripley, D. A. (1997). On the relation between NDVI, fractional vegetation cover, and leaf area index. *Remote Sensing of Environment*, 62(3), 241–252. [https://doi.org/10.1016/S0034-4257\(97\)00104-1](https://doi.org/10.1016/S0034-4257(97)00104-1)
- Clark, M. P., Fan, Y., Lawrence, D. M., Adam, J. C., Bolster, D., Gochis, D. J., et al. (2015). Improving the representation of hydrologic processes in earth system models. *Water Resources Research*, 51, 5929–5956. <https://doi.org/10.1002/2015WR017096>
- Clow, D. W. (2010). Changes in the timing of snowmelt and streamflow in Colorado: A response to recent warming. *Journal of Climate*, 23(9), 2293–2306. <https://doi.org/10.1175/2009JCLI2951.1>
- Cosme, L. H., Schiatti, J., Costa, F. R., & Oliveira, R. S. (2017). The importance of hydraulic architecture to the distribution patterns of trees in a central Amazonian forest. *New Phytologist*, 215(1), 113–125. <https://doi.org/10.1111/nph.14508>
- Daly, C., Halbleib, M., Smith, J. I., Gibson, W. P., Doggett, M. K., Taylor, G. H., et al. (2008). Physiographically sensitive mapping of climatological temperature and precipitation across the conterminous United States. *International Journal of Climatology: A Journal of the Royal Meteorological Society*, 28(15), 2031–2064. <https://doi.org/10.1002/joc.1688>
- Dobrowski, S. Z. (2011). A climatic basis for microrefugia: The influence of terrain on climate. *Global Change Biology*, 17(2), 1022–1035. <https://doi.org/10.1111/j.1365-2486.2010.02263.x>
- Famiglietti, J., Rudnicki, J., & Rodell, M. (1998). Variability in surface moisture content along a hillslope transect: Rattlesnake Hill, Texas. *Journal of Hydrology*, 210(1–4), 259–281. [https://doi.org/10.1016/S0022-1694\(98\)00187-5](https://doi.org/10.1016/S0022-1694(98)00187-5)
- Famiglietti, J., & Wood, E. (1994). Multiscale modeling of spatially variable water and energy balance processes. *Water Resources Research*, 30(11), 3061–3078. <https://doi.org/10.1029/94WR01498>
- Fan, Y. (2015). Groundwater in the Earth's critical zone: Relevance to large-scale patterns and processes. *Water Resources Research*, 51, 3052–3069. <https://doi.org/10.1002/2015WR017037>
- Fan, Y., Clark, M., Lawrence, D. M., Swenson, S., Band, L. E., Brantley, S. L., et al. (2019). Hillslope hydrology in global change research and earth system modeling. *Water Resources Research*, 55, 1737–1772. <https://doi.org/10.1029/2018WR023903>
- Fan, Y., Miguez-Macho, G., Jobbágy, E. G., Jackson, R. B., & Otero-Casal, C. (2017). Hydrologic regulation of plant rooting depth. *Proceedings of the National Academy of Sciences*, 114, 201712381. <https://doi.org/10.1073/pnas.1712381114>
- Fisher, R. A., Koven, C. D., Anderegg, W. R., Christoffersen, B. O., Dietze, M. C., Farris, C., et al. (2017). Vegetation demographics in earth system models: A review of progress and priorities. *Global Change Biology*, 24. <https://doi.org/10.1111/gcb.13910>
- Gamon, J. A., Field, C. B., Goulden, M. L., Griffin, K. L., Hartley, A. E., Joel, G., et al. (1995). Relationships between NDVI, canopy structure, and photosynthesis in three Californian vegetation types. *Ecological Applications*, 5(1), 28–41. <https://doi.org/10.2307/1942049>
- Glenn, E. P., Nagler, P. L., & Huete, A. R. (2010). Vegetation index methods for estimating evapotranspiration by remote sensing. *Surveys in Geophysics*, 31(6), 531–555. <https://doi.org/10.1007/s10712-010-9102-2>
- Gorelick, N., Hancher, M., Dixon, M., Ilyushchenko, S., Thau, D., & Moore, R. (2017). Google earth engine: Planetary-scale geospatial analysis for everyone. *Remote Sensing of Environment*, 202, 18–27. <https://doi.org/10.1016/j.rse.2017.06.031>
- Goulden, M., Anderson, R., Bales, R., Kelly, A., Meadows, M., & Winston, G. (2012). Evapotranspiration along an elevation gradient in California's Sierra Nevada. *Journal of Geophysical Research*, 117, G03028. <https://doi.org/10.1029/2012JG002027>
- Goulden, M., & Bales, R. (2019). California forest die-off linked to multi-year deep soil drying in 2012–2015 drought. *Nature Geoscience*, 12(8), 632–637. <https://doi.org/10.1038/s41561-019-0388-5>
- Guan, K., Pan, M., Li, H., Wolf, A., Wu, J., Medvigy, D., et al. (2015). Photosynthetic seasonality of global tropical forests constrained by hydroclimate. *Nature Geoscience*, 8(4), 284–289. <https://doi.org/10.1038/ngeo2382>
- Hirota, M., & Oliveira, R. (2020). Crossing thresholds on the way to ecosystem shifts. *Science*, 367(6479), 739–740. <https://doi.org/10.1126/science.aba7115>
- Hoylman, Z., Jencso, K., Hu, J., Holden, Z., Allred, B., & Dobrowski, S. (2019). The topographic signature of ecosystem climate sensitivity in the western United States. *Geophysical Research Letters*, 46, 14,508–14,508. <https://doi.org/10.1029/2019GL085546>
- Hoylman, Z. H., Jencso, K. G., Hu, J., Martin, J. T., Holden, Z. A., Seielstad, C. A., & Rowell, E. M. (2018). Hillslope topography mediates spatial patterns of ecosystem sensitivity to climate. *Journal of Geophysical Research: Biogeosciences*, 123, 353–371. <https://doi.org/10.1002/2017JG004108>
- Hu, J., Moore, D. J., Burns, S. P., & Monson, R. K. (2010). Longer growing seasons lead to less carbon sequestration by a subalpine forest. *Global Change Biology*, 16(2), 771–783. <https://doi.org/10.1111/j.1365-2486.2009.01967.x>
- Hu, J., Moore, D. J., Riveros-Iregui, D. A., Burns, S. P., & Monson, R. K. (2010). Modeling whole-tree carbon assimilation rate using observed transpiration rates and needle sugar carbon isotope ratios. *New Phytologist*, 185(4), 1000–1015. <https://doi.org/10.1111/j.1469-8137.2009.03154.x>
- Hwang, T., Band, L., & Hales, T. (2009). Ecosystem processes at the watershed scale: Extending optimality theory from plot to catchment. *Water Resources Research*, 45, W11425. <https://doi.org/10.1029/2009WR007775>
- Hwang, T., Band, L. E., Vose, J. M., & Tague, C. (2012). Ecosystem processes at the watershed scale: Hydrologic vegetation gradient as an indicator for lateral hydrologic connectivity of headwater catchments. *Water Resources Research*, 48, W06514. <https://doi.org/10.1029/2011WR011301>

- Jump, A. S., Ruiz-Benito, P., Greenwood, S., Allen, C. D., Kitzberger, T., Fensham, R., et al. (2017). Structural overshoot of tree growth with climate variability and the global spectrum of drought-induced forest dieback. *Global Change Biology*, *23*(9), 3742–3757. <https://doi.org/10.1111/gcb.13636>
- Kane, J. M., Kolb, T. E., & McMillin, J. D. (2014). Stand-scale tree mortality factors differ by site and species following drought in southwestern mixed conifer forests. *Forest Ecology and Management*, *330*, 171–182. <https://doi.org/10.1016/j.foreco.2014.06.042>
- Khanna, J., Medvigy, D., Fueglistaler, S., & Walko, R. (2017). Regional dry-season climate changes due to three decades of Amazonian deforestation. *Nature Climate Change*, *7*(3), 200–204. <https://doi.org/10.1038/nclimate3226>
- Klein, T., Randin, C., & Körner, C. (2015). Water availability predicts forest canopy height at the global scale. *Ecology Letters*, *18*(12), 1311–1320. <https://doi.org/10.1111/ele.12525>
- Konings, A., Williams, A., & Gentine, P. (2017). Sensitivity of grassland productivity to aridity controlled by stomatal and xylem regulation. *Nature Geoscience*, *10*(4), 284–288. <https://doi.org/10.1038/ngeo2903>
- Körner, C. (2007). The use of 'altitude' in ecological research. *Trends in Ecology & Evolution*, *22*(11), 569–574. <https://doi.org/10.1016/j.tree.2007.09.006>
- Li, Y., Guan, K., Gentine, P., Konings, A. G., Meinzer, F. C., Kimball, J. S., et al. (2017). Estimating global ecosystem isohydry/anisohydry using active and passive microwave satellite data. *Journal of Geophysical Research: Biogeosciences*, *122*, 3306–3321. <https://doi.org/10.1002/2017JG003958>
- Liu, Y., Kumar, M., Katul, G. G., & Porporato, A. (2019). Reduced resilience as an early warning signal of forest mortality. *Nature Climate Change*, *9*(11), 880–885. <https://doi.org/10.1038/s41558-019-0583-9>
- Lowry, J., Ramsey, R., Thomas, K., Schrupp, D., Sajwaj, T., Kirby, J., et al. (2007). Mapping moderate-scale land-cover over very large geographic areas within a collaborative framework: A case study of the southwest regional gap analysis project (SWReGAP). *Remote Sensing of Environment*, *108*(1), 59–73. <https://doi.org/10.1016/j.rse.2006.11.008>
- Lutz, J. A., Van Wagtenonk, J. W., & Franklin, J. F. (2010). Climatic water deficit, tree species ranges, and climate change in Yosemite National Park. *Journal of Biogeography*, *37*(5), 936–950. <https://doi.org/10.1111/j.1365-2699.2009.02268.x>
- Mackay, D. S. (2001). Evaluation of hydrologic equilibrium in a mountainous watershed: Incorporating forest canopy spatial adjustment to soil biogeochemical processes. *Advances in Water Resources*, *24*(9–10), 1211–1227. [https://doi.org/10.1016/S0309-1708\(01\)00040-9](https://doi.org/10.1016/S0309-1708(01)00040-9)
- Mackay, D. S., & Band, L. E. (1997). Forest ecosystem processes at the watershed scale: Dynamic coupling of distributed hydrology and canopy growth. *Hydrological Processes*, *11*(9), 1197–1217. [https://doi.org/10.1002/\(SICI\)1099-1085\(199707\)11:9<1197::AID-HYP552>3.0.CO;2-W](https://doi.org/10.1002/(SICI)1099-1085(199707)11:9<1197::AID-HYP552>3.0.CO;2-W)
- Magney, T. S., Bowling, D. R., Logan, B. A., Grossmann, K., Stutz, J., Blanken, P. D., et al. (2019). Mechanistic evidence for tracking the seasonality of photosynthesis with solar-induced fluorescence. *Proceedings of the National Academy of Sciences*, *116*(24), 11,640–11,645. <https://doi.org/10.1073/pnas.1900278116>
- Martin, J., Looker, N., Hoylman, Z., Jencso, K., & Hu, J. (2018). Differential use of winter precipitation by upper and lower elevation Douglas fir in the northern Rockies. *Global Change Biology*, *24*(12), 5607–5621. <https://doi.org/10.1111/gcb.14435>
- McLaughlin, B. C., Ackerly, D. D., Klos, P. Z., Natali, J., Dawson, T. E., & Thompson, S. E. (2017). Hydrologic refugia, plants, and climate change. *Global Change Biology*, *23*(8), 2941–2961. <https://doi.org/10.1111/gcb.13629>
- Millar, C. I., Stephenson, N. L., & Stephens, S. L. (2007). Climate change and forests of the future: Managing in the face of uncertainty. *Ecological Applications*, *17*(8), 2145–2151. <https://doi.org/10.1890/06-1715.1>
- Moeslund, J. E., Arge, L., Bøcher, P. K., Dalgaard, T., Ejrnæs, R., Odgaard, M. V., & Svenning, J.-C. (2013). Topographically controlled soil moisture drives plant diversity patterns within grasslands. *Biodiversity and Conservation*, *22*(10), 2151–2166. <https://doi.org/10.1007/s10531-013-0442-3>
- Moeslund, J. E., Arge, L., Bøcher, P. K., Dalgaard, T., & Svenning, J. C. (2013). Topography as a driver of local terrestrial vascular plant diversity patterns. *Nordic Journal of Botany*, *31*(2), 129–144. <https://doi.org/10.1111/j.1756-1051.2013.00082.x>
- Oliveira, R. S., Costa, F. R., van Baalen, E., de Jonge, A., Bittencourt, P. R., Almanza, Y., et al. (2019). Embolism resistance drives the distribution of Amazonian rainforest tree species along hydro-topographic gradients. *New Phytologist*, *221*(3), 1457–1465. <https://doi.org/10.1111/nph.15463>
- Pastorello, G., Papale, D., Chu, H., Trotta, C., Agarwal, D., Canfora, E., et al. (2017). The FLUXNET2015 dataset: The longest record of global carbon, water, and energy fluxes is updated. *Eos*, *98*.
- Rasmussen, C., Troch, P. A., Chorover, J., Brooks, P., Pelletier, J., & Huxman, T. E. (2011). An open system framework for integrating critical zone structure and function. *Biogeochemistry*, *102*(1–3), 15–29. <https://doi.org/10.1007/s10533-010-9476-8>
- R Core Team (2015). R: A language and environment for statistical computing. Vienna, Austria: R Foundation for Statistical Computing. <https://www.R-project.org/>
- Robinson, N. P., Allred, B. W., Jones, M. O., Moreno, A., Kimball, J. S., Naugle, D. E., et al. (2017). A dynamic Landsat derived normalized difference vegetation index (NDVI) product for the conterminous United States. *Remote Sensing*, *9*(8), 863. <https://doi.org/10.3390/rs9080863>
- Robinson, N. P., Allred, B. W., Smith, W. K., Jones, M. O., Moreno, A., Erickson, T. A., et al. (2018). Terrestrial primary production for the conterminous United States derived from Landsat 30 m and MODIS 250 m. *Remote Sensing in Ecology and Conservation*, *4*(3), 264–280. <https://doi.org/10.1002/rse2.74>
- Schwantes, A. M., Parolari, A. J., Swenson, J. J., Johnson, D. M., Domec, J.-C., Jackson, R. B., et al. (2018). Accounting for landscape heterogeneity improves spatial predictions of tree vulnerability to drought. *New Phytologist*, *220*(1), 132–146. <https://doi.org/10.1111/nph.15274>
- Simeone, C., Maneta, M. P., Holden, Z. A., Sapes, G., Sala, A., & Dobrowski, S. Z. (2018). Coupled ecohydrology and plant hydraulics modeling predicts ponderosa pine seedling mortality and lower treeline in the US Northern Rocky Mountains. *New Phytologist*, *221*. <https://doi.org/10.1111/nph.15499>
- Smith, L. A., Eissenstat, D. M., & Kaye, M. W. (2017). Variability in aboveground carbon driven by slope aspect and curvature in an eastern deciduous forest, USA. *Canadian Journal of Forest Research*, *47*(2), 149–158. <https://doi.org/10.1139/cjfr-2016-0147>
- Smith, W. K., Dannenberg, M. P., Yan, D., Herrmann, S., Barnes, M. L., Barron-Gafford, G. A., et al. (2019). Remote sensing of dryland ecosystem structure and function: Progress, challenges, and opportunities. *Remote Sensing of Environment*, *233*, 111401. <https://doi.org/10.1016/j.rse.2019.111401>
- Sun, Y., Frankenberger, C., Jung, M., Joiner, J., Guanter, L., Köhler, P., & Magney, T. (2018). Overview of solar-induced chlorophyll fluorescence (SIF) from the Orbiting Carbon Observatory-2: Retrieval, cross-mission comparison, and global monitoring for GPP. *Remote Sensing of Environment*, *209*, 808–823. <https://doi.org/10.1016/j.rse.2018.02.016>

- Swenson, S. C., Clark, M., Fan, Y., Lawrence, D. M., & Perket, J. (2019). Representing intrahillslope lateral subsurface flow in the community land model. *Journal of Advances in Modeling Earth Systems*, *11*(12), 4044–4065. <https://doi.org/10.1029/2019MS001833>
- Swetnam, T. L., Brooks, P. D., Barnard, H. R., Harpold, A. A., & Gallo, E. L. (2017). Topographically driven differences in energy and water constrain climatic control on forest carbon sequestration. *Ecosphere*, *8*(4). <https://doi.org/10.1002/ecs2.1797>
- Tague, C. L., Moritz, M., & Hanan, E. (2019). The changing water cycle: The eco-hydrologic impacts of forest density reduction in Mediterranean (seasonally dry) regions. *Wiley Interdisciplinary Reviews Water*, *6*(4), e1350. <https://doi.org/10.1002/wat2.1350>
- Tai, X., Mackay, D. S., Anderegg, W. R., Sperry, J. S., & Brooks, P. D. (2017). Plant hydraulics improves and topography mediates prediction of aspen mortality in southwestern USA. *New Phytologist*, *213*(1), 113–127. <https://doi.org/10.1111/nph.14098>
- Tai, X., Mackay, D. S., Ewers, B. E., Parsekian, A. D., Beverly, D., Speckman, H. N., et al. (2019). Plant hydraulic stress explained tree mortality and tree size explained beetle attack in a mixed conifer forest. *Journal of Geophysical Research: Biogeosciences*, *124*, 3555–3568. <https://doi.org/10.1029/2019JG005272>
- Tai, X., Mackay, D. S., Sperry, J. S., Brooks, P., Anderegg, W. R., Flanagan, L. B., et al. (2018). Distributed plant hydraulic and hydrological modeling to understand the susceptibility of riparian woodland trees to drought-induced mortality. *Water Resources Research*, *54*, 4901–4915. <https://doi.org/10.1029/2018WR022801>
- Thompson, S. E., Harman, C. J., Troch, P. A., Brooks, P. D., & Sivapalan, M. (2011). Spatial scale dependence of ecohydrologically mediated water balance partitioning: A synthesis framework for catchment ecohydrology. *Water Resources Research*, *47*, W00J03. <https://doi.org/10.1029/2010WR009998>
- Troch, P. A., Lahmers, T., Meira, A., Mukherjee, R., Pedersen, J. W., Roy, T., & Valdés-Pineda, R. (2015). Catchment coevolution: A useful framework for improving predictions of hydrological change? *Water Resources Research*, *51*, 4903–4922. <https://doi.org/10.1002/2015WR017032>
- Tromp-van Meerveld, H., & McDonnell, J. (2006). On the interrelations between topography, soil depth, soil moisture, transpiration rates and species distribution at the hillslope scale. *Advances in Water Resources*, *29*, 293–310. <https://doi.org/10.1016/j.advwatres.2005.02.016>
- Trujillo, E., Molotch, N. P., Goulden, M. L., Kelly, A. E., & Bales, R. C. (2012). Elevation-dependent influence of snow accumulation on forest greening. *Nature Geoscience*, *5*(10), 705–709. <https://doi.org/10.1038/ngeo1571>
- Tucker, C. J., Slayback, D. A., Pinzon, J. E., Los, S. O., Myneni, R. B., & Taylor, M. G. (2001). Higher northern latitude normalized difference vegetation index and growing season trends from 1982 to 1999. *International Journal of Biometeorology*, *45*(4), 184–190. <https://doi.org/10.1007/s00484-001-0109-8>
- Weintraub, S. R., Brooks, P. D., & Bowen, G. J. (2017). Interactive effects of vegetation type and topographic position on nitrogen availability and loss in a temperate montane ecosystem. *Ecosystems*, *20*(6), 1073–1088. <https://doi.org/10.1007/s10021-016-0094-8>
- Weintraub, S. R., Taylor, P. G., Porder, S., Cleveland, C. C., Asner, G. P., & Townsend, A. R. (2015). Topographic controls on soil nitrogen availability in a lowland tropical forest. *Ecology*, *96*(6), 1561–1574. <https://doi.org/10.1890/14-0834.1>
- Western, A. W., Grayson, R. B., Blöschl, G., Willgoose, G. R., & McMahon, T. A. (1999). Observed spatial organization of soil moisture and its relation to terrain indices. *Water Resources Research*, *35*(3), 797–810. <https://doi.org/10.1029/1998WR900065>
- Whittaker, R. H. (1967). Gradient analysis of vegetation. *Biological Reviews*, *42*(2), 207–264. <https://doi.org/10.1111/j.1469-185X.1967.tb01419.x>
- Zhu, Z., Wang, S., & Woodcock, C. E. (2015). Improvement and expansion of the Fmask algorithm: Cloud, cloud shadow, and snow detection for Landsats 4–7, 8, and Sentinel 2 images. *Remote Sensing of Environment*, *159*, 269–277. <https://doi.org/10.1016/j.rse.2014.12.014>
- Zscheischler, J., Mahecha, M. D., Von Buttlar, J., Harmeling, S., Jung, M., Rammig, A., et al. (2014). A few extreme events dominate global interannual variability in gross primary production. *Environmental Research Letters*, *9*(3), 035001. <https://doi.org/10.1088/1748-9326/9/3/035001>